Published for SISSA by Springer
Received: December 21, 2021
Revised: April 26, 2022
Accepted: July 14, 2022
Published: August 23, 2022

Explaining excesses in four-leptons at the LHC with a double peak from a CP violating Two Higgs Doublet Model

Stefan Antusch,[a] **Oliver Fischer,**[b] **A. Hammad**[c,d] **and Christiane Scherb**[e]

[a] *Department of Physics, University of Basel, Klingelbergstr. 82, Basel CH-4056, Switzerland*
[b] *Department of Mathematical Sciences, University of Liverpool, Liverpool L69 7ZL, U.K.*
[c] *Institute of Convergence Fundamental Studies, Seoul National University of Science and Technology, Seoul 01811, Korea*
[d] *Centre for Theoretical Physics, the British University in Egypt, P.O. Box 43, Cairo 11837, Egypt*
[e] *PRISMA$^+$ Cluster of Excellence & Mainz Institute for Theoretical Physics, Johannes Gutenberg University, Mainz 55099, Germany*

E-mail: stefan.antusch@unibas.ch, oliver.fischer@liverpool.ac.uk, ahmed.hammad@unibas.ch, cscherb@uni-mainz.de

Abstract: Extended scalar sectors with additional degrees of freedom appear in many scenarios beyond the Standard Model. Heavy scalar resonances that interact with the neutral current could be discovered via broad resonances in the tails of the four-lepton invariant mass spectrum, where the Standard Model background is small and well understood. In this article we consider a recent ATLAS measurement of four-lepton final states, where the data is in excess over the background for invariant masses above 500 GeV. We discuss the possibility that this excess could be interpreted as a "double peak" from the two extra heavy neutral scalars of a CP violating Two Higgs Doublet Model, both coupling to the Z boson. We apply an iterative fitting procedure to find viable model parameters that can match the excess, resulting in a benchmark point where the observed four-lepton invariant mass spectrum can be explained by two scalar particles H_2 and H_3, with masses of 544 GeV and 629 GeV, respectively, being admixtures of the CP eigenstates. Our explanation predicts additional production processes for $t\bar{t}$, W^+W^-, $4b$ and $\gamma\gamma$, some of which have cross sections close to the current experimental limits. Our results further imply that the electric dipole moment of the electron should be close to the present bounds.

Keywords: Phenomenological Models

ArXiv ePrint: 2112.00921

https://doi.org/10.1007/JHEP08(2022)224

Contents

JHEP08(2022)224

1 Introduction

The discovery of the scalar resonance with a mass of about 125 GeV, compatible with the predicted Higgs boson [1], completes the Standard Model (SM).

The ATLAS and CMS collaborations are now performing precision studies of SM processes, such as the production cross sections of top quark pairs [2, 3], and they continuously search for physics beyond the SM (BSM), for instance in final states with four b quarks [4], two tau leptons [5, 6], and two photons [7]. In addition, there are exotic searches for resonances, for instance in semileptonic final states [8].

While currently most searches for physics beyond the SM do not point at BSM physics, excesses in final states with leptons [11–13] and di-photons [14–17] indicate the possible existence of additional scalar degrees of freedom. The four-lepton final states are often referred to as the 'golden channel' when searching for heavy scalar resonances, due to small and controllable SM backgrounds. The four-lepton analyses from ATLAS [11] and CMS [18, 19] show enhanced event rates in final states with high invariant mass. These analyses were combined in ref. [10] wherein the compatibility of the data with a broad resonance structure around 700 GeV has been claimed. This is compatible with a very recent interpretation of ATLAS data as a second Higgs excitation at 680 GeV [20].

Searches for heavy scalars above 600 GeV in $\gamma\gamma$, $Z\gamma$, $ZZ \to 4\ell$, top quarks, pairs of Higgs and W bosons were reviewed and discussed in ref. [9], supporting the claim made in ref. [10] of a resonance in ZZ around 700 GeV. This possible resonant enhancement is visible both in gluon and vector boson fusion channels as reported by ATLAS in ref. [11]. The more recent analysis of four-lepton final states by the ATLAS collaboration also shows an enhancement of event rates with invariant masses above about 500 GeV [21]. This observation was considered in ref. [22] to corroborate the possible resonance around 700 GeV.

The theoretical framework was the Georgi-Machacek model and a cross section for the heavy resonance was found to be $\sim 160\,\text{fb}$. It is interesting to note that a broader enhancement of the $b\bar{b}b\bar{b}$ final state with invariant mass above 500 GeV is visible, which might be compatible with the observed 4ℓ excess from ref. [4]. On the other hand, a recent analysis searching for heavy diboson resonances in semi-leptonic final states is compatible with the SM prediction [8], however here the backgrounds are at a much higher level and might cover up a possible enhancement.

In this article we consider an explanation of the four-lepton excess at invariant masses above 500 GeV by a "double peak" from the two extra heavy neutral scalars of a CP violating Two Higgs Doublet Model (THDM), where the latter extends the scalar sector of the SM by an additional scalar $\text{SU}(2)_L$ doublet field [23]. Due to the violation of CP the two extra heavy neutral scalars can couple to ZZ and thus be observable in the four-lepton invariant mass spectrum via a "double peak". Recently, we studied a class of THDMs with CP violation in ref. [24], exploring the testability of CP violation at the LHC and evaluating the current constraints on the model parameters, pointing out the importance of the four-lepton final state as "discovery channel". We will make use of the results of [24] to find a viable set of model parameters that can match the current four-lepton excess. The article is structured as follows: in section 2 we briefly review the model framework, in section 3 we describe our analysis and discuss the results, and in section 4 we conclude.

2 The model

The THDM was first discussed in ref. [25] to discuss the phenomenon of CP violation in the scalar sector. For a comprehensive review we refer the reader e.g. to ref. [26]. In THDMs, the scalar sector contains two $\text{SU}(2)_L$-doublet fields, ϕ_1 and ϕ_2, with identical quantum numbers under the SM gauge symmetry group:

$$\phi_1 = \begin{pmatrix} \eta_1^+ \\ (v_1 + h_1 + ih_3)/\sqrt{2} \end{pmatrix} \quad \text{and} \quad \phi_2 = \begin{pmatrix} \eta_2^+ \\ (v_2 + h_2 + ih_4)/\sqrt{2} \end{pmatrix} . \tag{2.1}$$

The components h_i, $i = 1, \ldots, 4$, are real neutral fields, η_i^+, $i = 1, 2$ are complex charged fields, and v_i, $i = 1, 2$ are the vacuum expectation values (vevs). The most general Lagrangian density for the model can be decomposed as

$$\mathcal{L}_{\text{THDM}} = \mathcal{L}_{\text{SM,kin}} + \mathcal{L}_{\phi,\text{kin}} + V_\phi + Y_\phi \,, \tag{2.2}$$

where $\mathcal{L}_{\text{SM,kin}}$ denotes the kinetic terms for SM gauge fields and fermions, $\mathcal{L}_{\phi,\text{kin}}$ denotes the kinetic terms for the two scalar fields ϕ_i, $i = 1, 2$, V_ϕ denotes the scalar potential, and Y_ϕ contains the Yukawa terms that give rise to the couplings between the SM fermions and the scalar fields. The scalar potential with a softly broken Z_2 symmetry is given by

$$\begin{aligned} V_\phi = {} & m_{11}^2(\phi_1^\dagger\phi_1) + m_{22}^2(\phi_2^\dagger\phi_2) - \left[m_{12}^2(\phi_1^\dagger\phi_2) + \text{h.c.}\right] + \lambda_1(\phi_1^\dagger\phi_1)^2 + \lambda_2(\phi_2^\dagger\phi_2)^2 \\ & + \lambda_3(\phi_1^\dagger\phi_1)(\phi_2^\dagger\phi_2) + \lambda_4(\phi_1^\dagger\phi_2)(\phi_2^\dagger\phi_1) + \frac{1}{2}\left[\lambda_5(\phi_1^\dagger\phi_2)^2 + \text{H.c.}\right] . \end{aligned} \tag{2.3}$$

JHEP08(2022)224

The parameters $m_{ii}^2, \lambda_{i\neq 5}$ are real, and the possible complex phases of the two parameters $m_{12}^2 = |m_{12}^2|e^{i\eta(m_{12}^2)}$ and $\lambda_5 = |\lambda_5|e^{i\eta(\lambda_5)}$ allow for CP violation. The tadpole equations impose a relation between the two complex phases, such that the CP violation can be parametrised ultimately via the parameter $\eta(\lambda_5)$, the complex phase of λ_5. In the following, we will use η instead of $\eta(\lambda_5)$. Furthermore, we define $\tan\beta := v_2/v_1$, where v_i, $i = 1, 2$ is the vacuum expectation value of ϕ_i and $v = \sqrt{v_1^2 + v_2^2}$ for the SM vev $v \approx 246\,\text{GeV}$ is satisfied.

Since scalar decays into four-lepton final states (henceforth referred to as 4ℓ) come about from scalar decays into two Z bosons that in turn decay into leptons, we are interested in the interaction of the scalar fields with the neutral current. There are only two interaction eigenstates that can decay into two Z bosons. However, the most general (CP violating) form of the THDM leads to scalar mixing, and in the presence of CP violation all the three neutral mass eigenstates H_i of the THDM can mediate the process $pp \to H_i \to ZZ \to 4\ell$, with $i = 1, 2, 3$.

The final state from the process $pp \to H_i \to ZZ \to 4\ell$, with $4\ell = \ell_\alpha^+\ell_\alpha^-\ell_\beta^+\ell_\beta^-$ (and where the considered lepton flavors are $\ell_{\alpha,\beta}^\pm = e^\pm, \mu^\pm$) features an invariant mass that reflects the mass of the mediating H_i. The mass eigenstate H_1 corresponds to the SM-like Higgs boson with $m_{H_1} \simeq 125\,\text{GeV}$, whose four-lepton signal has been studied (see examples for ATLAS [27] and CMS [28] analyses) and H_2 and H_3 are assumed to be heavier. As discussed above, in a CP violating THDM the extra neutral scalars H_2 and H_3 give rise to two additional broad peaks in the 4ℓ invariant mass spectrum — or to a broad "double peak" if the masses are not too separated. These broad peaks are due to the interference of the scalars and their total decay widths, cf. figure 2 below. This is a feature that is usually not considered when fitting the THDM to the data.

3 Analysis and results

We consider the measurements of differential cross-sections in 4ℓ events in the $139\,\text{fb}^{-1}$ data set by the ATLAS collaboration [21]. From the results in the ATLAS publication we use the 4ℓ differential cross sections, and in particular the invariant mass spectrum ($M_{4\ell}$). We digitise the observed event rates, their errors, and the theory prediction.

We use the eight bins from $M_{4\ell}$ between 500 GeV and 900 GeV, six of which show event counts in excess of the theory prediction. We create a sample of excess events by subtracting the theory prediction from the observed event rates (which means that "excess events" per bin can also be negative).

Notice that a similar analysis by the CMS collaboration exists, where the 4ℓ differential cross section was extracted from $35.9\,\text{fb}^{-1}$ data [29]. As this data set is much smaller than the ATLAS one, we shall not use it in our analysis. We discuss below it's compatibility with our results.

3.1 Numerical setup

As an explicit example we consider the same class of THDMs with CP violation and type I Yukawa structure as in ref. [24], to which we refer the reader for model details and notation.

JHEP08(2022)224

We calculate testable properties of the THDM via numerical tools that include the following recent constraints:[1] B physics data using FlavorKit [30], and electric dipole moments with the formulae from refs. [31, 32].

We include constraints from the global data set on the Higgs boson, with the latest results from the LHC experiments. The data is combined with the numerical tool HiggsBounds-5.3.2 [33–35] and HiggsSignals-2.2.3 [35–37]. The lightest boson in our model, H_1, takes on the role of the Higgs boson in the SM, and is constrained by state-of-the art signal rate and mass measurements. Thus our parameter space points are ensured to have an SM-like Higgs boson in the spectrum, which limits the amount of mixing between the two Higgs doublets.

The inclusive process $pp \to H_2, H_3 \to 4\ell$ for the heavy scalars is calculated in MadGraph [38], including the effective gluon-Higgs vertex via SPheno [39, 40] and QCD corrections [41]. We note at this point that the inclusive 4ℓ invariant mass spectrum is simulated to include the interference between the scalars. A fast detector simulation is done with 500k events per sample with Delphes [42] using the standard ATLAS detector card. From the reconstructed events we read out the invariant mass spectra.

3.2 First approximation

We searched for points with masses m_{H_2} and m_{H_3} around 500 GeV and 700 GeV, respectively, and with total cross sections for the 4ℓ final state that are of similar magnitude. We found the benchmark point P_1 with $m_{H_2}^{P_1} = 535\,\text{GeV}$ and $m_{H_3}^{P_1} = 703\,\text{GeV}$ and total 4ℓ cross sections $\sigma_{H_2\to 4\ell}^{P_1} = 1.3\,\text{fb}$ and $\sigma_{H_3\to 4\ell}^{P_1} = 0.86\,\text{fb}$. For H_2 and H_3 the signal selection efficiency based on the experimental selection criteria is found to be $\epsilon_{4\ell} \sim 0.3$ and not too dependent on the scalar mass. We simulated exclusively $pp \to H_2 \to 4\ell$ and $pp \to H_3 \to 4\ell$ from which we obtained the invariant mass spectra ρ_2 and ρ_3, respectively. Notice that at this step, the interference between the scalars is not taken into account.

Next we performed a simple χ^2 analysis. We varied the signal peaks of the two spectra with the two parameters δm_j, such that the masses are given by $m_{H_j} = m_{H_j}^{P_1} + \delta m_j$. We also introduce the signal strength multipliers s_j which are multiplied with the invariant mass spectra ρ_{H_j}. We construct the χ^2:

$$\chi^2_{\text{sig}}(\delta m_2, \delta m_3, s_2, s_3) = \sum_i \frac{(b_{\text{sig},i}(\delta m_2, \delta m_3, s_2, s_3) - b_i)^2}{\delta^2_{\text{obs},i} + \delta^2_{sys,i}} \tag{3.1}$$

where i is the bin number, b_i is the measured event rate $\delta_{\text{obs},i} = \sqrt{b_i}$, $\delta_{\text{syst},i} = 10\%$, corresponding to the uncertainty quoted in the ATLAS analysis. The signal rate for bin i is

$$b_{\text{sig},i}(\delta m_2, \delta m_3, s_2, s_3) = b_{\text{SM},i} + \int_i (s_2 \cdot \rho_{H_2}(E - \delta m_2) + s_3 \cdot \rho_{H_3}(E - \delta m_3))dE\,, \tag{3.2}$$

with $b_{\text{SM},i}$ being the SM prediction, ρ_{H_j} the signal distributions, and the parameters δm_j and s_j are varied to minimise the χ^2.

[1] We use the same limits as detailed in section 3 of ref. [24].

JHEP08(2022)224

3.3 Iterative analysis

Notice that the signal rate as described in eq. (3.2) distorts the invariant mass spectrum and thus disconnects it from the underlying benchmark point. However, the distorted spectrum can be used to locate the masses and event rates that are preferred by the fit to the data.

Consequently we use the best-fit values for the masses and the total 4ℓ cross sections (converted from the fiducial cross sections using the signal selection efficiency and the integrated luminosity) as selection criteria to find a new benchmark point. From a fine grained scan in the model parameters we select a point P_n that has masses m_{H_j} and cross sections $\sigma_{H_j\to 4\ell}$ that are as close to the best-fit results for the masses and event rates of the previous point P_{n-1} as possible.

For each new point P_n we create an inclusive 4ℓ invariant mass spectrum $\rho^{P_n}_{\text{incl}}$ with two peaks around m_{H_2} and m_{H_3}, including the interference between H_2 and H_3. We remark that the interference with H_1 is negligible for the here relevant mass scales of H_2 and H_3, which we verified by computation. We separate the spectrum into $\rho^{P_n}_{H_2}$ and $\rho^{P_n}_{H_3}$ at the minimum between the two peaks and fit the parameters δm_j and s_j via the two partial spectra as in eq. (3.1) to the data.

Once we have a benchmark point with a spectrum that provides a good fit, we carry out a Bayesian fit of the parameters δm_j, $j = 2, 3$ and s_j, $j = 2, 3$ to establish the Bayesian confidence limits on the parameters.

3.4 Results

Our analysis converged sufficiently after six iterations. We perform an even more fine-grained parameter space scan and select parameter space points with m_{H_2}, m_{H_3}, $\sigma_{H_2\to 4\ell}$ and $\sigma_{H_3\to 4\ell}$ within the 90% Bayesian confidence interval around the last iteration's best fit parameters, which are:

$$\begin{aligned} 521.1\,\text{GeV} \le m_{H_2} \le 562.9\,\text{GeV}, \qquad & 602.2\,\text{GeV} \le m_{H_3} \le 655.9\,\text{GeV}, \\ 0.6\,\text{fb} \le \sigma_{\text{tot}} \le 1.2\,\text{fb}, \qquad & 0.5 \le r \le 2.0 \end{aligned} \tag{3.3}$$

where we introduced the total signal strength $\sigma_{\text{tot}} = \sigma_{pp\to H_2,H_3\to 4\ell}$ and the relative signal strength $r = b_{\text{sig},2}/b_{\text{sig},3}$ via the ratio of the quantity defined in eq. (3.2). We perform an even more fine-grained parameter space scan and select parameter space points with masses m_{H_2}, m_{H_3}, inclusive signal cross section $\sigma_{pp\to H_2,H_3\to 4\ell}$ and the relative signal strength r to be consistent with the 90% Bayesian confidence interval above.[2] We approximate the ratio parameter $r = \sigma_2/\sigma_3$, where σ_i are the exclusive signal strengths for $pp \to H_i \to 4\ell$.

In this scan we find the benchmark point P_7 that is defined by the following model parameters: $\tan\beta = 21$, $\eta = 0.663$, $\lambda_1 = 0.73$, $\lambda_2 = 0.099$, $\lambda_3 = 4.76$, $\lambda_4 = 6.45$ and $\Re(\lambda_5) = 1.63$. These parameters give rise to $m^{P_7}_{H_2} = 544\,\text{GeV}$, $m^{P_7}_{H_3} = 629\,\text{GeV}$, and $\sigma^{P_7}_{\text{tot}} = 0.77\,\text{fb}$, $r = 1.17\,\text{fb}$. We call this point the "best-fit benchmark point" as is provides

[2] We continue to use the Higgs signal strength constraints as input to our parameter space scan rather than adding the them to our χ^2, since we do not aim at statistical statements about which model is preferred by the data, as argued below.

JHEP08(2022)224

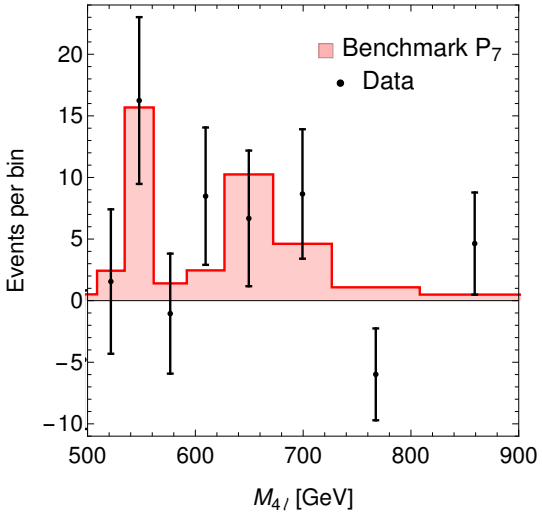

Figure 1. Invariant mass spectrum of the best-fit points for the "best-fit benchmark point" P_7, for details, see text. The black dots with error bars denote the difference between observed and predicted data from the four-lepton invariant mass spectrum in ref. [21].

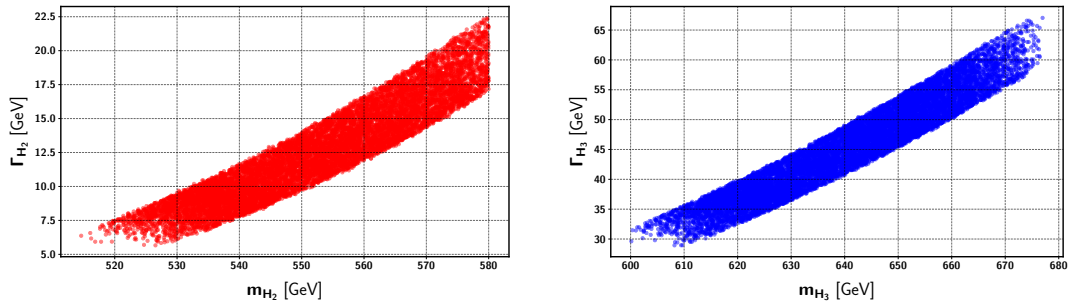

Figure 2. Total decay widths for the scalars H_2 and H_3, obtained from the very fine grained parameter space scan.

a very good fit to the spectrum with a $\chi^2 = 5.76$, which is to be compared to the SM value for all bins above 500 GeV. For the SM we get a $\chi^2_{\rm SM} = 21.0$ (16.9) corresponding to an upward fluctuation with a p-value of 0.007 (0.03) considering statistical errors only (all errors). The contribution of the two neutral scalar particles to the four-lepton invariant mass spectrum for the "best fit benchmark point" P_7 is shown in figure 1. The striking feature of the spectrum is the wide range of $M_{4\ell}$ that receives contributions from the two heavy scalars. This stems partly from their widths, which are $\mathcal{O}(10)$ GeV and $\mathcal{O}(50)$ GeV for H_2 and H_3, respectively, as shown in figure 2, and also from their interference.

The contribution of the two neutral scalar particles to the four-lepton invariant mass spectrum for the "best fit benchmark point" P_7 is shown in figure 1. The striking feature of the spectrum is the wide range of $M_{4\ell}$ that receives contributions from the two heavy scalars.

In general, scalars that mix with the Higgs doublet can also decay into other SM particles than Z bosons. Thus, after finding a good benchmark point to match the 4ℓ

JHEP08(2022)224

invariant mass spectrum as reported by ATLAS and CMS, we explore the possibility of making quantitative predictions for the H_i decays into $t\bar{t}$, W^+W^-, and $\gamma\gamma$. Therefore, we show in the four panels of figure 3 the projections of the different inclusive cross sections for the ~ 10000 parameter space points from the very fine grained scan over THDM model parameters. The figure includes the inclusive cross sections for W^+W^- (upper panels), $t\bar{t}$ (middle pannels) and $\gamma\gamma$ (lower panels), with the color code denoting the numerical value for $\sigma_{pp\to H_2,H_3\to 4\ell}$. The panels for WW and $\gamma\gamma$ include the current experimental limits from ref. [8] and ref. [7], respectively, denoted by the blue dashed lines.

3.5 Discussion

Our "best-fit benchmark point" P_7 provides an excellent fit to the excesses of events in the 4ℓ spectrum with invariant masses between 500 GeV and 700 GeV observed by the ATLAS collaboration. The fit prefers H_2 and H_3 with similar masses and contributions to the inclusive cross section for the 4ℓ final state. Combined with the facts that (i) the THDM adds one CP-even and one CP-odd scalar to the SM field content and (ii) that the CP-odd field does not decay into ZZ this implies that the mass eigenstates must be strongly CP-mixed. Indeed, selecting all parameter space points from our very fine-grained scan that are within the 90% Bayesian confidence interval of our fit in (3.3), we find that η lies in the range $0.63 \leq \eta \leq 0.68$. The CP properties of the two scalars could be tested at the HL-LHC via correlations in final states with two tau leptons from the processes $pp \to H_i \to \tau^+\tau^-$ as discussed in ref. [24].

A comment on the statistical meaning of our analysis is in order at this point. Clearly the current data set cannot be interpreted as more than a hint for the THDM. Furthermore, the large mass window leads to a large look elsewhere effect, which reduces the significance further. Ultimately, to establish a global significance for the THDM, higher statistics in the 4 lepton data and possibly also in the other channels are required. Additionally the scalar H_1, which is (slightly) different from the SM Higgs boson, has to be included into the fit as well. The central aim of this article is, however, *not* to establish statistical evidence for the existence of a THDM signal in the $M_{4\ell}$ spectrum. We rather want to point out that *if* the here discussed signal were to become statistically significant, the THDM with CP violation is a suitable candidate model to explain it.

CMS 4ℓ spectrum: we also investigated the compatibility of our best-fit benchmark point with the CMS four lepton spectrum from ref. [29]. This spectrum stems from an analysis of the CMS data set with $35.9\,\text{fb}^{-1}$, which is about one quarter of the ATLAS data set of $139\,\text{fb}^{-1}$. In the here considered range, between 500 and 900 GeV, the spectrum is subdivided into 23 bins with non-zero event counts, most of which have only one event with error bars that are larger than 1 event. Including this smaller data set into our analysis would dilute the statistical significance of our result if the CMS bins are treated on the same footing as the ATLAS bins. We calculated the theory prediction based on our best-fit benchmark point, and we find that it is compatible with the CMS data, with a $\chi^2/dof = 23/23$ [compared to 10/23 in the SM, mostly driven from the "s2" part of the signal]. This shows that the CMS data has little statistical weight compared to the ATLAS

JHEP08(2022)224

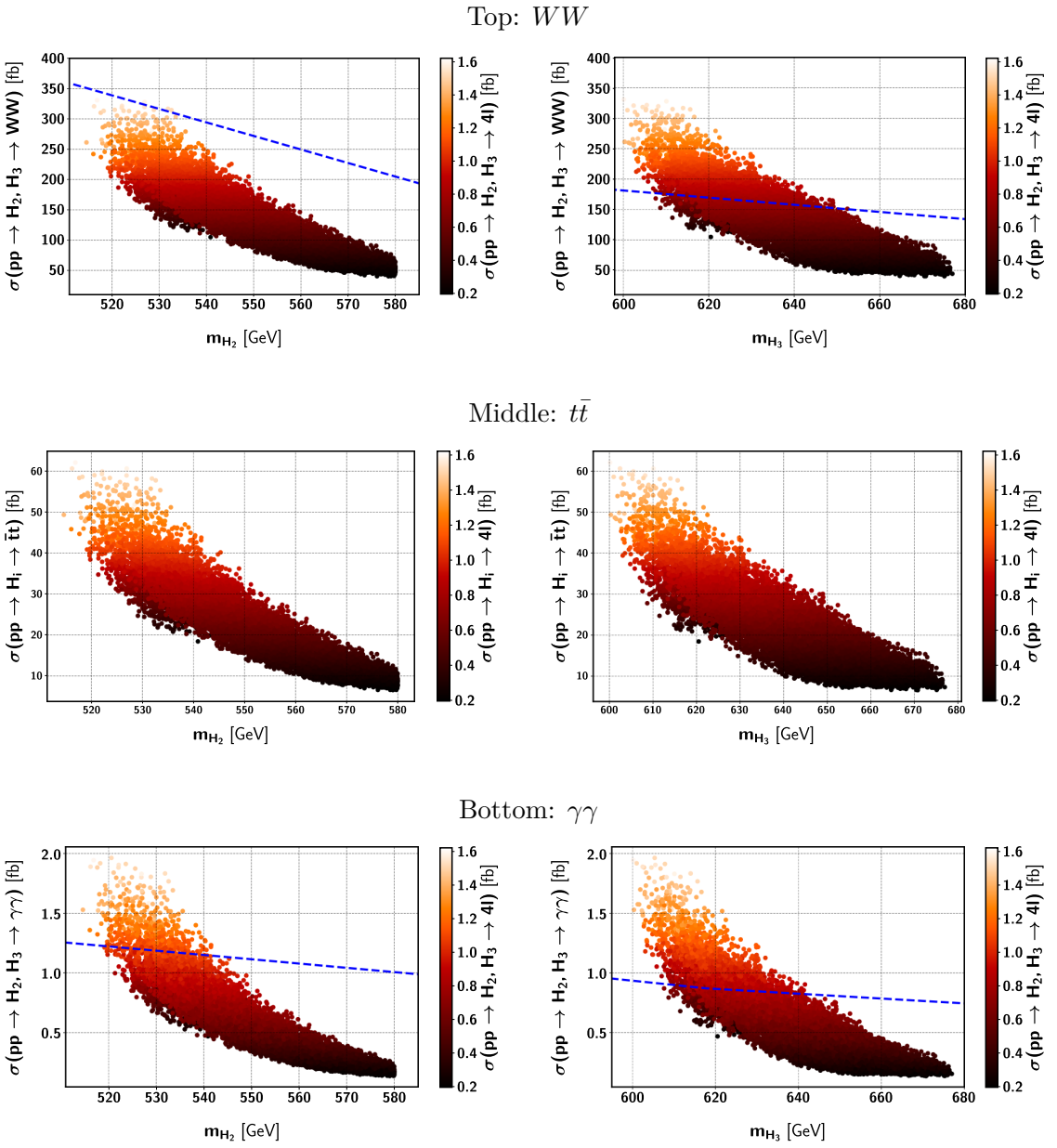

Figure 3. Results from a very fine-grained parameter space scan within the class of THDMs with CP violation and type I Yukawa structure (cf. [24]). Shown points feature masses m_{H_i} and inclusive cross sections $\sigma_{pp\to H_2,H_3\to 4\ell}$ within the 90% Bayesian confidence limit of the best-fit point. The left and right panels are for H_2 and H_3, respectively. *Top panel*: showing the W^+W^- final state with the blue dashed line denoting the 90% upper limit on the semileptonic cross section from ATLAS [8] for comparison. *Middle panel*: showing the $t\bar{t}$ final state. *Bottom panel*: showing the $\gamma\gamma$ final state with the dashed blue line denoting the 90% upper limits from ATLAS [7].

JHEP08(2022)224

data (obviously due to the data sample being smaller), which is why we did not include it into our fitting procedure.

Ditop channel: as mentioned above, our analysis allows us to make quantitative predictions for contributions of H_i, $i = 2, 3$ to the $t\bar{t}$ final state. Our "best-fit benchmark point" has the inclusive cross section $\sigma_{pp\to H_2,H_3\to t\bar{t}} = 28.3\,\text{fb}$. This — and actually also the cross sections from all the other points in our fine-grained scan — is much smaller than the current uncertainty of the recent measurements of the total production cross section $\sigma_{t\bar{t}} = 830 \pm 36\,(\text{stat}) \pm 14\,(\text{syst})\,\text{pb}$ by ATLAS [2] and $791 \pm 25\,\text{pb}$ by CMS [3].

Semi leptonic WW channel: let us now confront our "best-fit benchmark point" with the fact that no enhancement of semi-leptonic final states from WW or ZZ decays has been reported in ref. [8]. For our "best-fit benchmark point", the sum of WW and ZZ cross sections yields:

$$\sum_{V=W,Z} \sigma_{pp\to H_2,H_3\to VV} = 330\,\text{fb}\,. \tag{3.4}$$

This cross section is comparable with the 2σ upper limits on the production cross section from ref. [8], which are about 250 fb and 150 fb for scalar bosons with masses of 560 GeV and 640 GeV, respectively (for the example of a scalar radion). We note that V quadruplet production processes like $pp \to H_{j>1} \to 2H_1 + X \to 4V + X$ may have substantially increased cross sections and could become relevant signal channels in the future [43].

$4b$ channel: the small apparent enhancement of the $b\bar{b}b\bar{b} = 4b$ final state for invariant masses above 500 GeV as observed in ref. [4] could be another indication for the process $pp \to H_2, H_3 \to ZZ$. For the corresponding cross section one would expect that

$$\sigma_{pp\to H_2,H_3\to 4b} \geq \left(\frac{\text{Br}(Z\to b\bar{b})}{\text{Br}(Z\to \ell^+\ell^-)}\right)^2 \epsilon_b^4 \frac{\epsilon_{4b}}{\epsilon_{4\ell}} \tag{3.5}$$

with the b-tagging efficiency $\epsilon_b \simeq 0.7$, and the selection efficiencies $\epsilon_{4b} \sim 0.1$, and where additional $4b$ production could come from $pp \to H_i \to 2H_1 \to 4b$. Eq. (3.5) results in a lower limit of 16.5 additional events in the $4b$ final state, which matches quite well the observed ~ 20 events in excess of the background for $M_{4b} \geq 500\,\text{GeV}$.

Diphoton channel: next we comment on the $pp \to H_2, H_3 \to \gamma\gamma$ channel, for which our "best-fit benchmark point" has the inclusive cross section $\sigma_{pp\to H_2,H_3\to\gamma\gamma} = 0.8\,\text{fb}$. The ATLAS search for resonances in diphoton final states limits the production cross section to be less 1.15 fb and 0.83 fb at 2σ, for resonances with masses corresponding to 544 GeV and 629 GeV, respectively [7]. This implies that our "best-fit benchmark point" is only slightly in tension (at 1σ) with the ATLAS limits, but may still be regarded as compatible. We also note that in the current data there indeed exist some upward fluctuations of the observed event counts at 540 GeV and at 680 GeV. In any case, future analyses of the diphoton spectrum with more data should be able to test this prediction of our "best-fit benchmark point".

JHEP08(2022)224

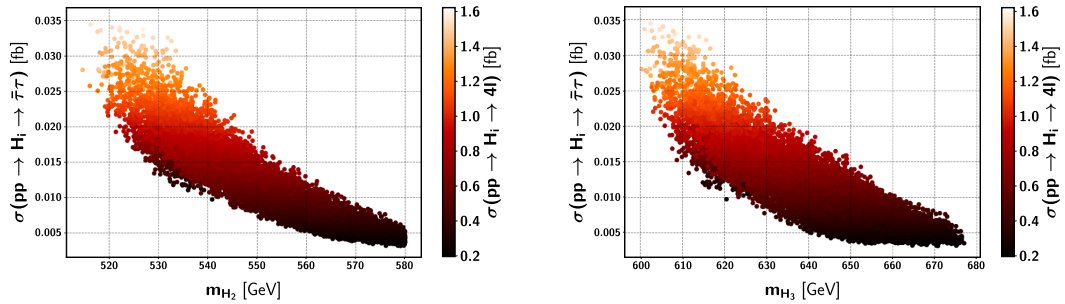

Figure 4. Results from the very fine-grained parameter space scan for the inclusive production cross section of $\tau^+\tau^-$ via H_2 and H_3.

Ditau channel: the heavy scalars H_2 and H_3 can give rise to resonances in the invariant mass spectrum of $\tau^+\tau^-$ final states, for which our "best-fit benchmark point" has a cross section of 0.015 fb. Such resonances have been searched for by ATLAS [5] and CMS [6]. No hints for additional τ production has been found with recent limits of $\sigma_{\tau\tau} < \mathcal{O}(100)$ $[\mathcal{O}(1)]$ fb for resonances around 500 [1000] GeV. We show the resulting predictions for the inclusive production cross section $\sigma_{pp\to H_2,H_3\to\tau^+\tau^-}$ in figure 4, which makes clear that our benchmark points are not likely to produce an observable signal in this final state.

Electric dipole moments: last but not least we consider the impact that CP violation in the scalar sector has for low-energy observables. As mentioned above, large CP-violating phases are an implication from H_2 and H_3 having similar signal strengths in the 4ℓ final state. Large CP phases imply that the THDM fields give rise to the Electric Dipole Moments (EDM) of SM particles, in particular for the electron. Both H_2 and H_3 contribute to the EDM via Barr-Zee diagrams, cf. e.g. refs. [31, 32, 44] and ref. [45] for the two-loop calculation. In the type-I THDM all fermions couple to ϕ_2 leading to the couplings being proportional to $\frac{1}{\tan\beta}$. On the other hand, fermion couplings to ϕ_1 (e.g. down-type quarks and leptons in the type-II THDM) are proportional to $\tan\beta$ [46]. Here, we generally consider large $\tan\beta$ so that the new contributions to the EDM are suppressed. For our fine-grained parameter space scan we calculate the EDM of every point according to the formulae from refs. [31, 32] and reject EDM for the electrons that are above the current exclusion limit from the ACME collaboration $|d_e| < 1.1 \times 10^{-29}$ ecm [47], cf. figure 5. We find that the majority ($\gtrsim 90\%$) of all points has $10^{-30} \leq \frac{|d_e|}{\text{ecm}} \leq 1.09 \cdot 10^{-29}$.

4 Conclusions

In this paper we have considered a "double peak" from a CP violating Two Higgs Doublet Model as explanation for the local excess in four-lepton events with invariant masses above 500 GeV as observed by ATLAS and CMS. Within a class of THDMs, we used an iterative fitting procedure to search for model parameters that give rise to heavy Higgs masses and signal strengths towards explaining the excess.

JHEP08(2022)224

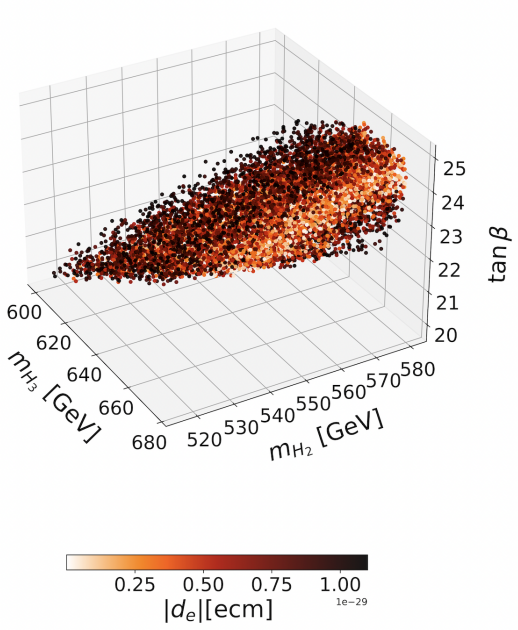

Figure 5. Parameter space points from the very fine grained scan, projected over the two masses and $\tan\beta$. The color code denotes the magnitude of the electron dipole moment d_e.

The "best-fit benchmark point" (called P_7) we found this way provides an excellent explanation for the ATLAS with a $\chi^2 = 5.76$ for 8 bins, predicting events in excess of the SM in the range from 500 GeV to around 700 GeV, and it also agrees with the statistically less relevant CMS data. It prefers a broad "double peak" in the invariant mass spectrum, with two resonances at 544 GeV and 629 GeV, respectively.

Interpreted in the context of a THDM, our results would be an indication for CP violation in the scalar sector. The CP mixing is required to be close to maximal due to the comparable signal strength in invariant mass ranges relating to the masses of H_2 and H_3. Currently the signal strength in this channel is too weak, but the CP mixing of H_2 and H_3 could in principle be tested at the HL-LHC in the future, e.g. via the di-tau final state (cf. [24]).

Our "best-fit benchmark point" predicts additional $t\bar{t}$, VV and $\gamma\gamma$ production channels with inclusive cross sections of about 28 fb for $t\bar{t}$, 159 fb for WW and 0.8 fb for $\gamma\gamma$. Our results are compatible with present limits, and may be responsible for minor excesses in the $4b$ and $\gamma\gamma$ channels. Moreover, the parameter space that leads to an explanation of the observed 4ℓ spectrum gives rise to electron EDMs that are close to the current experimental bounds, providing an example for a complementary way to test the scenario by low energy experiments.

Acknowledgments

This work was supported by the Swiss National Science Foundation. A. Hammad is supported from the Basic Science Research Program through the National Research Founda-

JHEP08(2022)224

tion of Korea Research Grant No. NRF-2021R1A2C4002551. CS was supported by the Cluster of Excellence Precision Physics, Fundamental Interactions, and Structure of Matter (PRISMA+ EXC 2118/1) funded by the German Research Foundation (DFG) within the German Excellence Strategy (Project ID 39083149), and by grant 05H18UMCA1 of the German Federal Ministry for Education and Research (BMBF).

JHEP08(2022)224

References

[1] ATLAS and CMS collaborations, *Measurements of the Higgs boson production and decay rates and constraints on its couplings from a combined ATLAS and CMS analysis of the LHC pp collision data at $\sqrt{s} = 7$ and 8 TeV*, *JHEP* **08** (2016) 045 [arXiv:1606.02266] [INSPIRE].

[2] ATLAS collaboration, *Measurement of the $t\bar{t}$ production cross-section in the lepton+jets channel at $\sqrt{s} = 13$ TeV with the ATLAS experiment*, *Phys. Lett. B* **810** (2020) 135797 [arXiv:2006.13076] [INSPIRE].

[3] CMS collaboration, *Measurement of differential $t\bar{t}$ production cross sections in the full kinematic range using lepton+jets events from proton-proton collisions at $\sqrt{s} = 13$ TeV*, *Phys. Rev. D* **104** (2021) 092013 [arXiv:2108.02803] [INSPIRE].

[4] ATLAS collaboration, *Search for the $HH \to b\bar{b}b\bar{b}$ process via vector-boson fusion production using proton-proton collisions at $\sqrt{s} = 13$ TeV with the ATLAS detector*, *JHEP* **07** (2020) 108 [*Erratum JHEP* **01** (2021) 145] [*Erratum JHEP* **05** (2021) 207] [arXiv:2001.05178] [INSPIRE].

[5] ATLAS collaboration, *Search for heavy Higgs bosons decaying into two tau leptons with the ATLAS detector using pp collisions at $\sqrt{s} = 13$ TeV*, *Phys. Rev. Lett.* **125** (2020) 051801 [arXiv:2002.12223] [INSPIRE].

[6] CMS collaboration, *Search for heavy resonances decaying to tau lepton pairs in proton-proton collisions at $\sqrt{s} = 13$ TeV*, *JHEP* **02** (2017) 048 [arXiv:1611.06594] [INSPIRE].

[7] ATLAS collaboration, *Search for resonances decaying into photon pairs in 139 fb^{-1} of pp collisions at $\sqrt{s} = 13$ TeV with the ATLAS detector*, *Phys. Lett. B* **822** (2021) 136651 [arXiv:2102.13405] [INSPIRE].

[8] ATLAS collaboration, *Search for heavy diboson resonances in semileptonic final states in pp collisions at $\sqrt{s} = 13$ TeV with the ATLAS detector*, *Eur. Phys. J. C* **80** (2020) 1165 [arXiv:2004.14636] [INSPIRE].

[9] F. Richard, *Indications for extra scalars at LHC? BSM physics at future e^+e^- colliders*, arXiv:2001.04770 [INSPIRE].

[10] P. Cea, *Evidence of the true Higgs boson H_T at the LHC Run 2*, *Mod. Phys. Lett. A* **34** (2019) 1950137 [arXiv:1806.04529] [INSPIRE].

[11] ATLAS collaboration, *Search for heavy ZZ resonances in the $\ell^+\ell^-\ell^+\ell^-$ and $\ell^+\ell^-\nu\bar{\nu}$ final states using proton-proton collisions at $\sqrt{s} = 13$ TeV with the ATLAS detector*, *Eur. Phys. J. C* **78** (2018) 293 [arXiv:1712.06386] [INSPIRE].

[12] W. Abdallah, S. Khalil and S. Moretti, *Double Higgs peak in the minimal SUSY $B-L$ model*, *Phys. Rev. D* **91** (2015) 014001 [arXiv:1409.7837] [INSPIRE].

[13] S. Buddenbrock et al., *The emergence of multi-lepton anomalies at the LHC and their compatibility with new physics at the EW scale*, *JHEP* **10** (2019) 157 [arXiv:1901.05300] [INSPIRE].

[14] CMS collaboration, *Search for new resonances in the diphoton final state in the mass range between* 70 *and* 110 *GeV in pp collisions at* $\sqrt{s} = 8$ *and* 13 *TeV*, CMS-PAS-HIG-17-013 (2017).

[15] P.J. Fox and N. Weiner, *Light Signals from a Lighter Higgs*, *JHEP* **08** (2018) 025 [arXiv:1710.07649] [INSPIRE].

[16] U. Haisch and A. Malinauskas, *Let there be light from a second light Higgs doublet*, *JHEP* **03** (2018) 135 [arXiv:1712.06599] [INSPIRE].

[17] T. Biekötter, M. Chakraborti and S. Heinemeyer, *The "96 GeV excess" at the LHC*, *Int. J. Mod. Phys. A* **36** (2021) 2142018 [arXiv:2003.05422] [INSPIRE].

[18] CMS collaboration, *Measurements of properties of the Higgs boson in the four-lepton final state at* $\sqrt{s} = 13$ *TeV*, CMS-PAS-HIG-18-001 (2018).

[19] CMS collaboration, *Measurements of properties of the Higgs boson decaying into four leptons in pp collisions at* $\sqrt{s} = 13$ *TeV*, CMS-PAS-HIG-16-041 (2016).

[20] M. Consoli and L. Cosmai, *Experimental signals for a second resonance of the Higgs field*, *Int. J. Mod. Phys. A* **37** (2022) 2250091 [arXiv:2111.08962] [INSPIRE].

[21] ATLAS collaboration, *Measurements of differential cross-sections in four-lepton events in* 13 *TeV proton-proton collisions with the ATLAS detector*, *JHEP* **07** (2021) 005 [arXiv:2103.01918] [INSPIRE].

[22] F. Richard, *Global interpretation of LHC indications within the Georgi-Machacek Higgs model*, talk presented at the *International Workshop on Future Linear Colliders (LCWS2021)*, online, Switzerland, 15–18 March 2021, arXiv:2103.12639 [INSPIRE].

[23] H.E. Haber, G.L. Kane and T. Sterling, *The Fermion Mass Scale and Possible Effects of Higgs Bosons on Experimental Observables*, *Nucl. Phys. B* **161** (1979) 493 [INSPIRE].

[24] S. Antusch, O. Fischer, A. Hammad and C. Scherb, *Testing CP Properties of Extra Higgs States at the HL-LHC*, *JHEP* **03** (2021) 200 [arXiv:2011.10388] [INSPIRE].

[25] T.D. Lee, *A Theory of Spontaneous T Violation*, *Phys. Rev. D* **8** (1973) 1226 [INSPIRE].

[26] G.C. Branco, P.M. Ferreira, L. Lavoura, M.N. Rebelo, M. Sher and J.P. Silva, *Theory and phenomenology of two-Higgs-doublet models*, *Phys. Rept.* **516** (2012) 1 [arXiv:1106.0034] [INSPIRE].

[27] ATLAS collaboration, *Higgs boson production cross-section measurements and their EFT interpretation in the* 4ℓ *decay channel at* $\sqrt{s} = 13$ *TeV with the ATLAS detector*, *Eur. Phys. J. C* **80** (2020) 957 [*Erratum ibid.* **81** (2021) 29] [*Erratum ibid.* **81** (2021) 398] [arXiv:2004.03447] [INSPIRE].

[28] CMS collaboration, *Measurements of production cross sections of the Higgs boson in the four-lepton final state in proton-proton collisions at* $\sqrt{s} = 13$ *TeV*, *Eur. Phys. J. C* **81** (2021) 488 [arXiv:2103.04956] [INSPIRE].

JHEP08(2022)224

[29] CMS collaboration, *Search for a new scalar resonance decaying to a pair of Z bosons in proton-proton collisions at* $\sqrt{s} = 13$ *TeV*, *JHEP* **06** (2018) 127 [*Erratum JHEP* **03** (2019) 128] [arXiv:1804.01939] [INSPIRE].

[30] W. Porod, F. Staub and A. Vicente, *A Flavor Kit for BSM models*, *Eur. Phys. J. C* **74** (2014) 2992 [arXiv:1405.1434] [INSPIRE].

[31] T. Abe, J. Hisano, T. Kitahara and K. Tobioka, *Gauge invariant Barr-Zee type contributions to fermionic EDMs in the two-Higgs doublet models*, *JHEP* **01** (2014) 106 [*Erratum JHEP* **04** (2016) 161] [arXiv:1311.4704] [INSPIRE].

[32] E.J. Chun, J. Kim and T. Mondal, *Electron EDM and Muon anomalous magnetic moment in Two-Higgs-Doublet Models*, *JHEP* **12** (2019) 068 [arXiv:1906.00612] [INSPIRE].

[33] P. Bechtle et al., *HiggsBounds-4: Improved Tests of Extended Higgs Sectors against Exclusion Bounds from LEP, the Tevatron and the LHC*, *Eur. Phys. J. C* **74** (2014) 2693 [arXiv:1311.0055] [INSPIRE].

[34] P. Bechtle, S. Heinemeyer, O. Stal, T. Stefaniak and G. Weiglein, *Applying Exclusion Likelihoods from LHC Searches to Extended Higgs Sectors*, *Eur. Phys. J. C* **75** (2015) 421 [arXiv:1507.06706] [INSPIRE].

[35] https://higgsbounds.hepforge.org/downloads.

[36] P. Bechtle, S. Heinemeyer, O. Stål, T. Stefaniak and G. Weiglein, *HiggsSignals: Confronting arbitrary Higgs sectors with measurements at the Tevatron and the LHC*, *Eur. Phys. J. C* **74** (2014) 2711 [arXiv:1305.1933] [INSPIRE].

[37] P. Bechtle, S. Heinemeyer, O. Stål, T. Stefaniak and G. Weiglein, *Probing the Standard Model with Higgs signal rates from the Tevatron, the LHC and a future ILC*, *JHEP* **11** (2014) 039 [arXiv:1403.1582] [INSPIRE].

[38] J. Alwall et al., *The automated computation of tree-level and next-to-leading order differential cross sections, and their matching to parton shower simulations*, *JHEP* **07** (2014) 079 [arXiv:1405.0301] [INSPIRE].

[39] W. Porod, *SPheno, a program for calculating supersymmetric spectra, SUSY particle decays and SUSY particle production at* e^+e^- *colliders*, *Comput. Phys. Commun.* **153** (2003) 275 [hep-ph/0301101] [INSPIRE].

[40] W. Porod and F. Staub, *SPheno 3.1: Extensions including flavour, CP-phases and models beyond the MSSM*, *Comput. Phys. Commun.* **183** (2012) 2458 [arXiv:1104.1573] [INSPIRE].

[41] A. Belyaev, N.D. Christensen and A. Pukhov, *CalcHEP 3.4 for collider physics within and beyond the Standard Model*, *Comput. Phys. Commun.* **184** (2013) 1729 [arXiv:1207.6082] [INSPIRE].

[42] DELPHES 3 collaboration, *DELPHES 3, A modular framework for fast simulation of a generic collider experiment*, *JHEP* **02** (2014) 057 [arXiv:1307.6346] [INSPIRE].

[43] N. Darvishi and M.R. Masouminia, *Signature of the Maximally Symmetric 2HDM via* $W^{\pm}/Z$*-Quadruplet Productions at the LHC*, *Phys. Rev. D* **103** (2021) 095031 [arXiv:2012.14746] [INSPIRE].

[44] K. Cheung, A. Jueid, Y.-N. Mao and S. Moretti, *Two-Higgs-doublet model with soft CP violation confronting electric dipole moments and colliders*, *Phys. Rev. D* **102** (2020) 075029 [arXiv:2003.04178] [INSPIRE].

JHEP08(2022)224

[45] W. Altmannshofer, S. Gori, N. Hamer and H.H. Patel, *Electron EDM in the complex two-Higgs doublet model*, *Phys. Rev. D* **102** (2020) 115042 [arXiv:2009.01258] [INSPIRE].

[46] D. Egana-Ugrinovic and S. Thomas, *Higgs Boson Contributions to the Electron Electric Dipole Moment*, arXiv:1810.08631 [INSPIRE].

[47] ACME collaboration, *Improved limit on the electric dipole moment of the electron*, *Nature* **562** (2018) 355 [INSPIRE].

[48] ATLAS collaboration, *Search for dijet resonances in events with an isolated charged lepton using $\sqrt{s} = 13$ TeV proton-proton collision data collected by the ATLAS detector*, *JHEP* **06** (2020) 151 [arXiv:2002.11325] [INSPIRE].

JHEP08(2022)224